Supplementary Information

Intermedium aminophenol enables hectogram-scale synthesis of highly-bright red carbon quantum dots at ambient condition

Xiangyong Meng, Maorong Wang, Jishuai Lin, Lihua Wang, Jin Liu, Yang Song*, Qiang Jing*, Haiguang Zhao*

College of Materials Science and Engineering, College of Textiles and Clothes, College of Physics, State Key Laboratory of Bio-Fibers and Eco-Textiles, Qingdao University, No. 308 Ningxia Road, Qingdao 266071, P. R. China.

*Corresponding authors.

E-mail: yangsong@qdu.edu.cn; jingq@qdu.edu.cn; hgzhao@qdu.edu.cn.

ORCID: Yang Song: 0000-0002-0050-4570; Qiang Jing: 0000-0001-7590-2613; Haiguang Zhao: 0000-0003-1057-9522; Xiangyong Meng: 0009-0005-2488-6824.

1. Experimental Procedures

1.1 Synthesis of R-C-dots

R-C-dots were synthesized in an open environment. First, completely dissolved 5 g of o-PDA (Shanghai Maclean's Biochemical Technology Co., Ltd., 99.5% purity) in 100 mL of deionized water were transferred into a beaker and stirred at 60 °C for 2 h. Next, the pH of the solution was adjusted to 5-6 using acid, such as sulfuric acid, hydrochloric acid or citric acid. The solution was heated at 60 °C for another 10 h. Finally, the solution was cooled to room temperature at ambient conditions, and vacuum filtration was applied to the solution to obtain solid powder of R-C-dots. Furthermore, impurity was removed by cleaning multiple times using hot deionized water. Finally, the R-C-dots were dispersed in ethanol and further purified though dialysis (molecular weight cut-off ¼ 1000 Da) for characterizations.

1.2 Preparation of Red Phosphor

Firstly, 1 mg of R-C-dots powder and 500 mg of PVP was dissolved in 20 mL of ethanol. Then, stirring the mixture for 2 h to mix R-C-dots well

with PVP. Finally, the obtained solution was dried to obtain R-C-dots/PVP solid, and then R-C-dots/PVP powder was obtained by grinding.

1.3 Fabrication of WLED with R-C-dots/PVP Phosphor

Firstly, R-C-dots/PVP and YAG phosphors (Shenzhen looking long technology co., LTD) with mass ratio of 2:1 were thoroughly ground for even blending, and then a specific amount of epoxy resin AB glue was used to paint the R-C-dots/PVP/YAG phosphors onto a blue LED chip (450 nm, Shenzhen looking long technology co., LTD) to fabricate the WLED. Finally, the WLED was stationary for 12 h to cure the phosphor layer. The WLED was trigged by 3 mA, direct current. The HPCS-320 spectral color luxmeter (Hangzhou Hongpoo Light & Color Technology Co., Ltd) was used to characterize the optical properties of the WLED.

1.4 Density Functional Theory Calculations

The theoretical calculations were performed via the Gaussian 16 suite of programs. The structures of the studied molecules were fully optimized at the B3LYP-D3BJ/6-311G(d) level of theory. The solvent effect was included in the calculations using the solvation model based on the density (SMD) model. The vibrational frequencies of the optimized structures were carried out at the same level. The structures were characterized as a local energy minimum on the potential energy surface by verifying that all the vibrational frequencies were real. The Gibbs free

energies of the optimized structures were calculated at the same level.

1.5 The procedure for two-photon absorption (TPA) cross sections measurements

First, the TPA coefficient (β, in unit of cm GW^{-1}) of the samples were measured using open-aperture Z-scan technique. Femtosecond pulses from a Mai-Tai laser (80 MHz, 100 fs, Spectra-Physics, Inc.), with tunable wavelength range from 660 to 1060 nm, were used as the excitation source. During the measurements, a beam splitter was used to divide the incident beam into two parts. The first part was served as the reference, while the other was focused by a circular lens with 30 cm focus length into a 1 mm thick quartz cuvette filled with the sample solutions. Then, the TPA cross sections (σ, in unit of GM) of the samples were estimated according to the following equation:

$$\sigma = 1000\beta h\nu/(N_A d_0)$$

in which NA is the Avogadro's number. d0 is the molar concentration of the sample (in units of M L^{-1}), while hν is the incident photon energy.

1.6 Measurement method for the photostability of R-C-dots

First, 1 mg of R-C-dots powder is evenly dispersed in 10 ml of ethanol to form the sample. Next, A UV lamp with a wavelength of 395 nm was selected as the light source to excite the sample. Further, adjust the UV light intensity to 100 mW/cm^2 on the sample surface. Finally, record the

fluorescence intensity of the sample (The integrated area of PL spectra from 550 nm to 750 nm) at one-second intervals.

1.7 Characterization methods

A transmission electron microscope (TEM, JEM-2100F) showed the morphologies of R-C-dots. Composition of R-C-dots, aminophenol, and intermediate were analyzed using X-ray photoelectron spectroscopy (XPS, Axis Supra+). The XRD pattern of R-C-dots was obtained via X-ray diffraction with Cu Kα radiation (Rigaku Smartlab, 3KW). HR-MS analyses were measured via high-performance liquid chromatography-mass spectrometry (LCMS-2020), in which the mobile phase was ethanol, and the separation products were ionized in the electrospray ionization (ESI) and operated in positive mode. NMR analyses were performed with a nuclear magnetic resonance spectroscopy (NMR, BRUKERAVANCE III HD 600MHz). FTIR spectra were performed with a Thermo-Fisher spectrometer (ESCALAB Xi+). The PLQY and lifetime of R-C-dots was measured by steady-state transient fluorescence spectrometer (FLS1000). PL spectra were recorded by Near infrared steady-state transient fluorescence spectrometer (Fluorolog-QM) and UV-vis absorption spectra were recorded by ultraviolet-visible NIR Spectrophotometer (PE Lambad750). The exciton dynamics of R-C-dots was studied using time resolved ultra-fast transient absorption (TA) spectroscopy (ultrafast

system- helios).

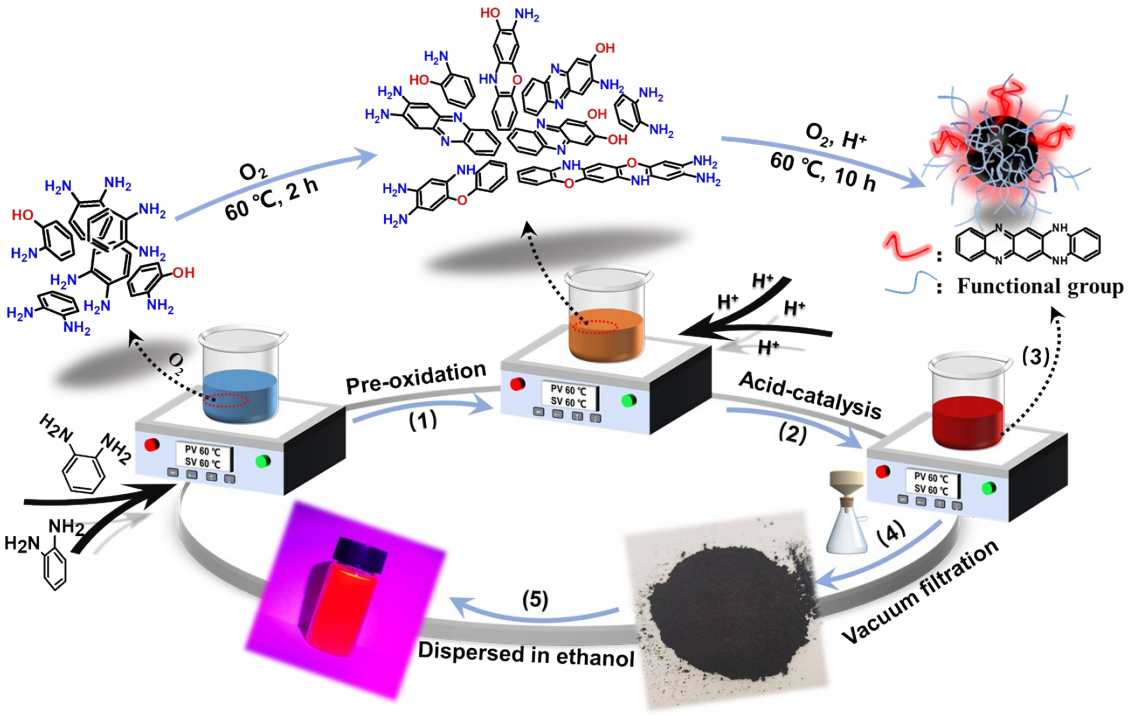

Figure S1. Schematic diagram of the synthesis of R-C-dots.

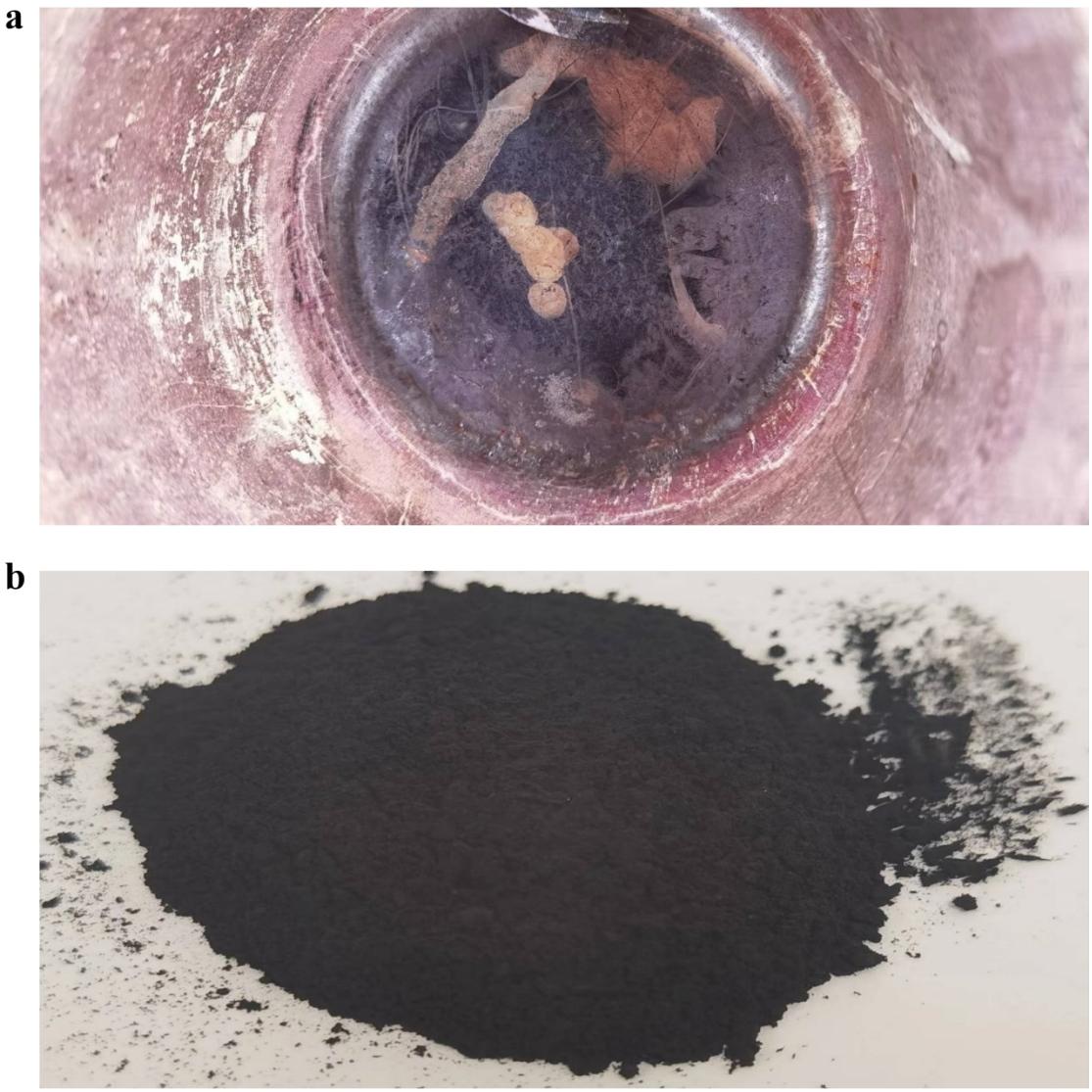

Figure S2. Image of R-C-dots before vacuum filtration. (a) The beaker used for the reaction is lined with a large amount of R-C-dots powder, as well as (b) a solid powder of R-C-dots obtained by vacuum filtration.

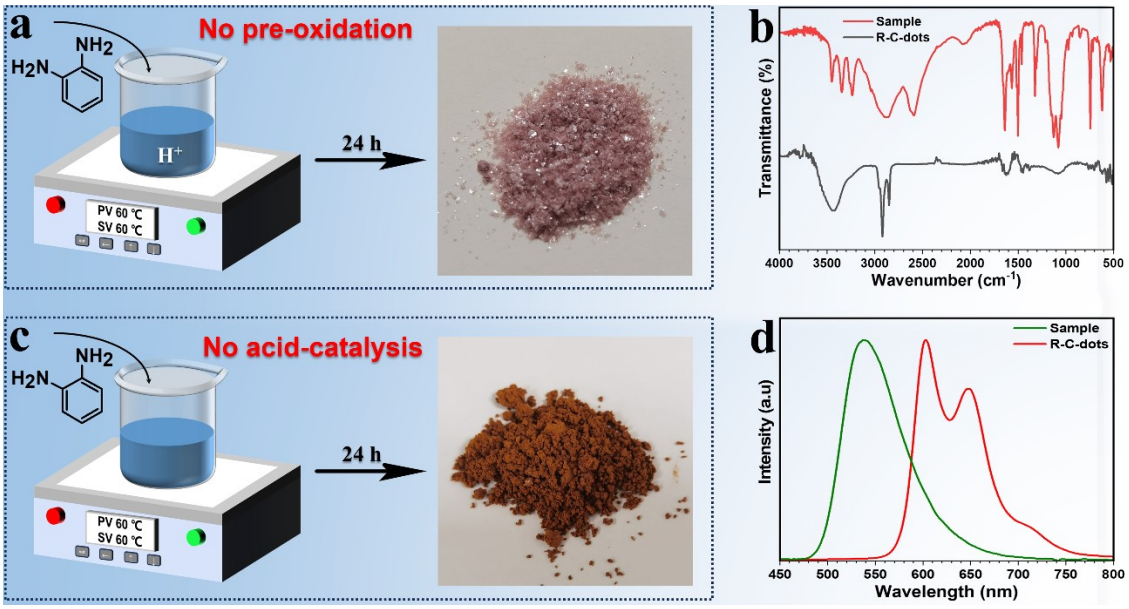

Figure S3. The schematic diagrams of the two sets of experiments. (a) o-PDA solution was heated at 60 °C for 24 h under acidic conditions (inset is image of obtained sample), and (b) FTIR spectra of the sample (black line) and R-C-dots (red line). The different FTIR spectra between the product and the R-C-dots proved that the product was not R-C-dots. (c) o-PDA solution was heated at 60 ℃ for 24 h (inset is image of obtained sample), and (d) PL spectra of the sample (green line) and R-C-dots (red line). The difference in the appearance and PL spectra evidenced that the product was not R-C-dots.

Table S1. A series of experiments using AP and o-PDA as precursors. The reaction temperature was 60 °C, and the pH range of acid-catalysis was 5 to 6.

Group	Precursor	Pre-oxidation	Acid-catalysis	R-C-dots
1	o-PDA	No	10 h	No
2	o-PDA	10 h	No	No
3	AP and o-PDA	No	10 h	Yes
4	o-PDA	2 h	10 h	Yes
5	AP	2 h	10 h	No
6	AP	10 h	No	No
7	AP and o-PDA	10 h	No	No

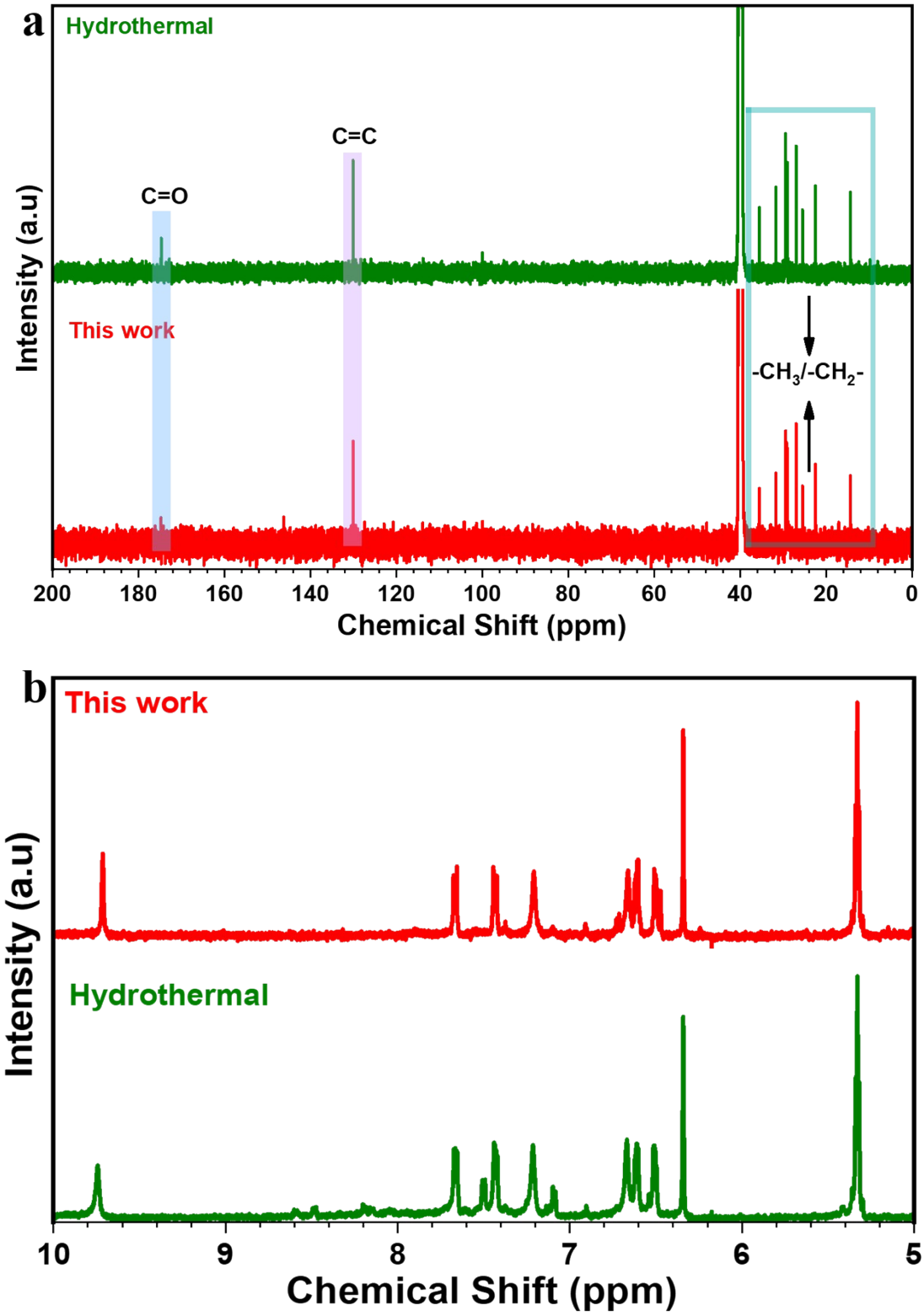

Figure S4. (a) ^{13}C NMR spectrum of H-R-C-dots (green line) and R-C-dots (red line). (b) ^{1}H NMR spectrum of H-R-C-dots (green line) and R-

C-dots (red line).

Table S2. Effect of the different pH about acid-catalysis on the yield of R-C-dots. The reaction temperature was 60 °C, the pre-oxidation time was 2 h, the pH range was 5 to 6, and the acid-catalysis was 10 h.

Group	pH	R-C-dots	Yield (%)
1	1-2	No	/
2	3-4	Yes	05 %
3	5-6	Yes	077 %
4	7-8	No	/

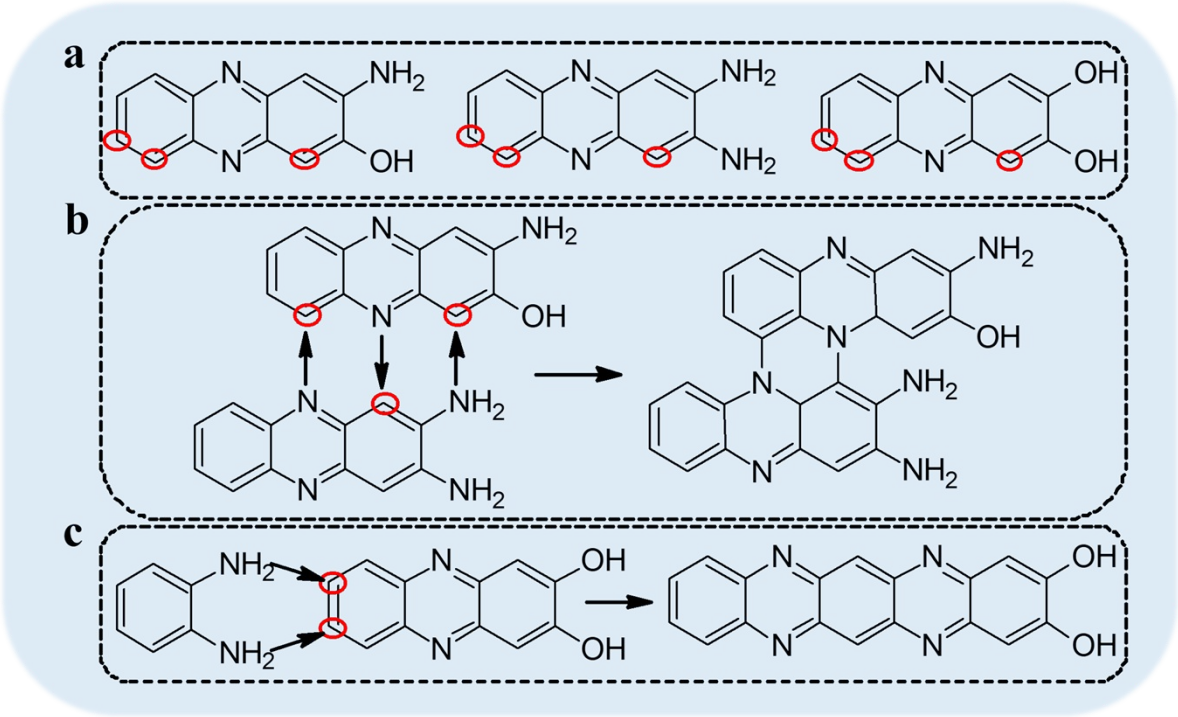

Figure S5. Schematic diagram of the reaction process in a low pH condition. (a) When highly protonated, the active site for intermediates were activated (red circle). (b) Schematic diagram of the network aggregation reaction. (c) Schematic diagram of a chain polymerization reaction.

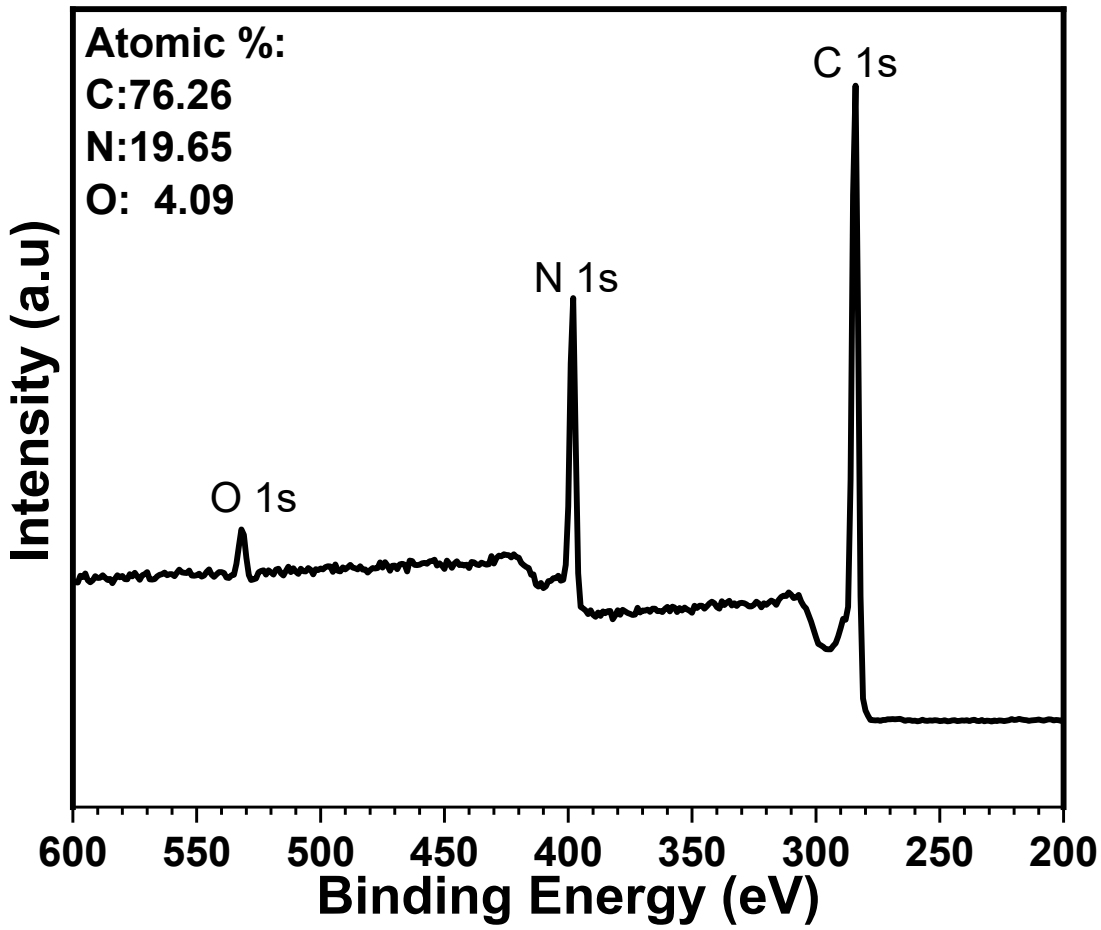

Figure S6. Full-scan XPS spectrum of sample 2h.

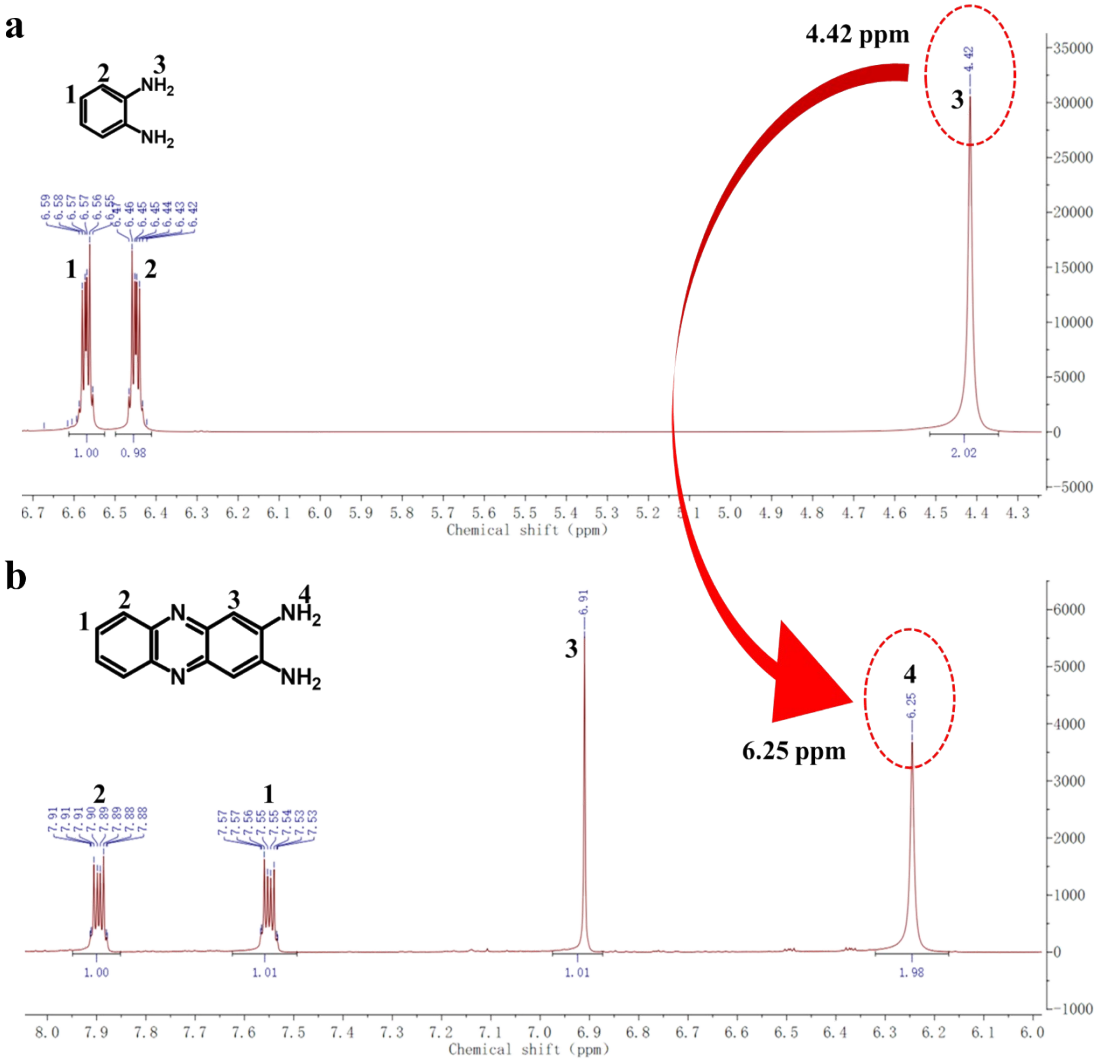

Figure S7. NMR spectra of o-PDA and DAP. (a) ^{1}H NMR spectrum of o-PDA, and (b) ^{1}H NMR spectrum of DAP.

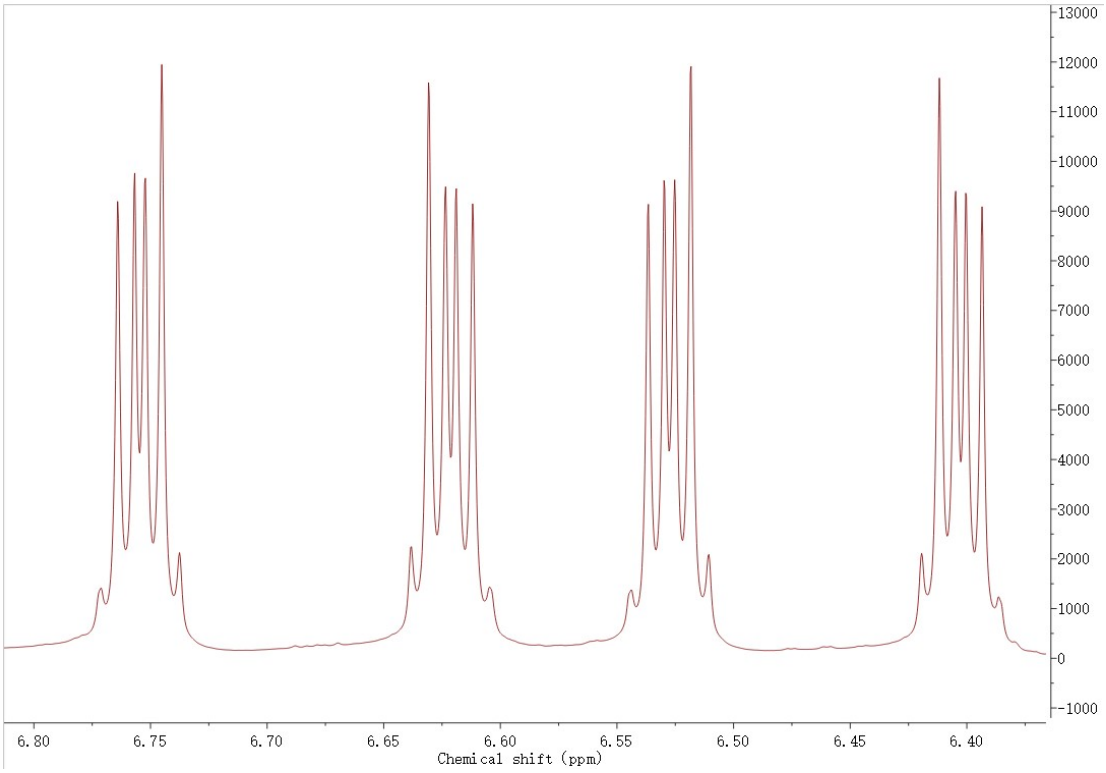

Figure S8. ^{1}H NMR spectrum of sample from 6.35-6.8 ppm.

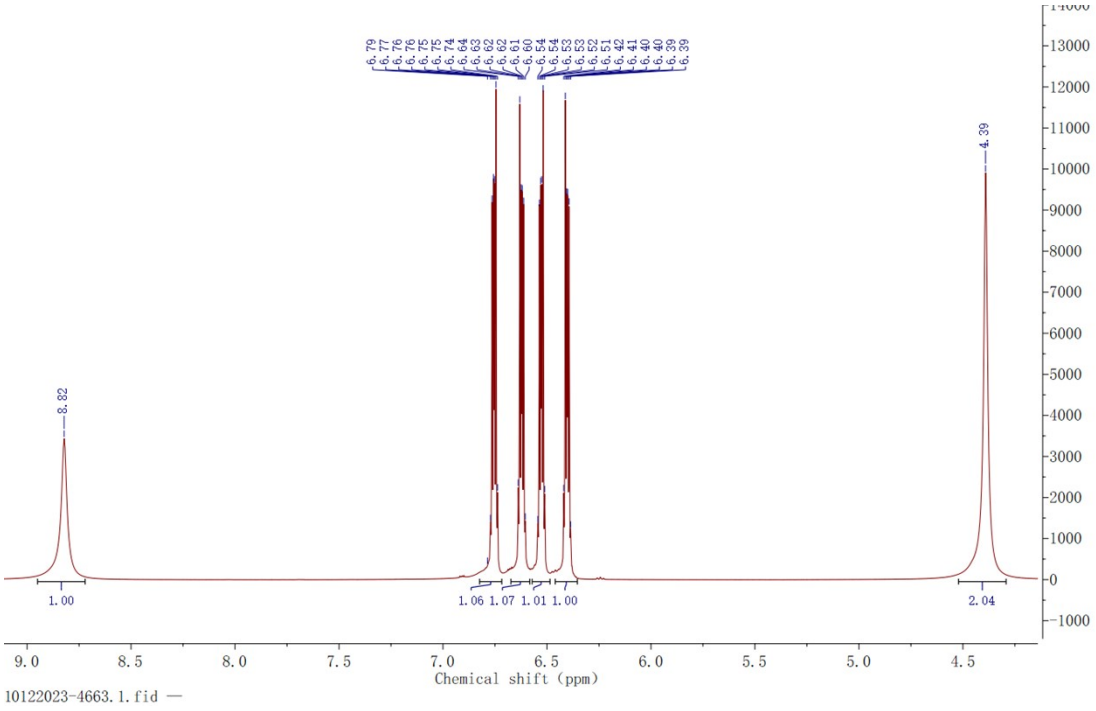

Figure S9. ^{1}H NMR spectrum of sample 2h with integral area from 4.39 ppm to 8.82 ppm.

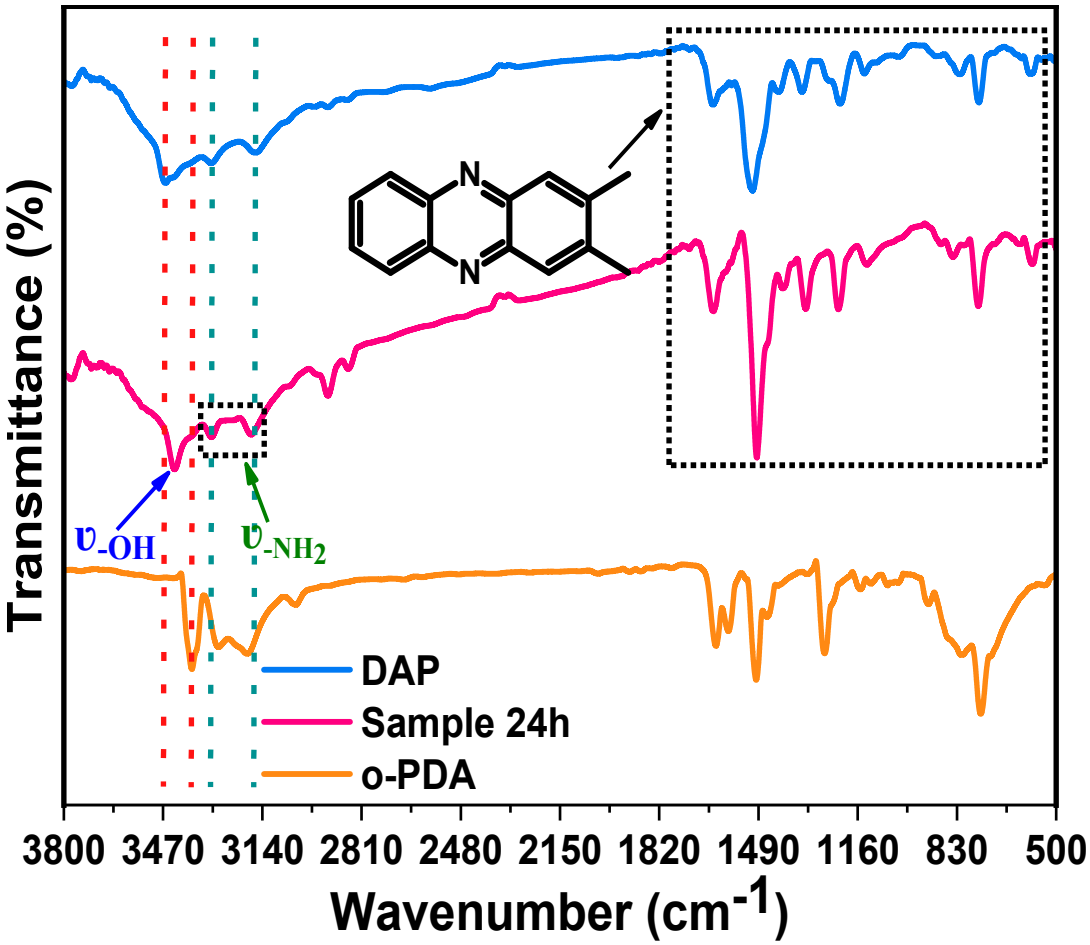

Figure S10. FTIR spectra of sample 24h (red line), DAP (blue line), and o-PDA (orange line).

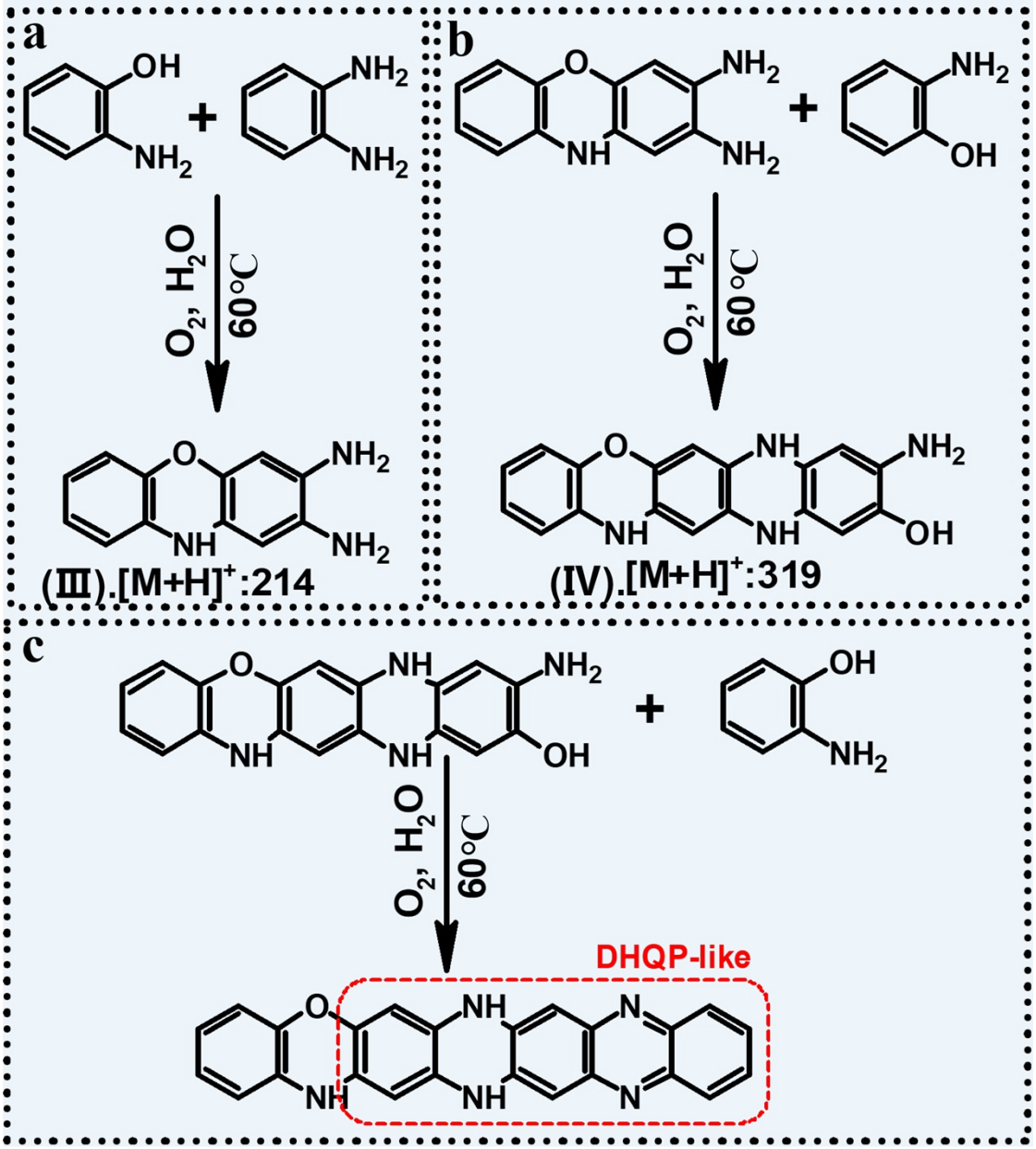

Figure S11. Schematic diagram of DHQP-like structure formation. (a), (b) The formation process of I and II, respectively. (c) DHQP-like structure was formed by reaction of IV with AP.

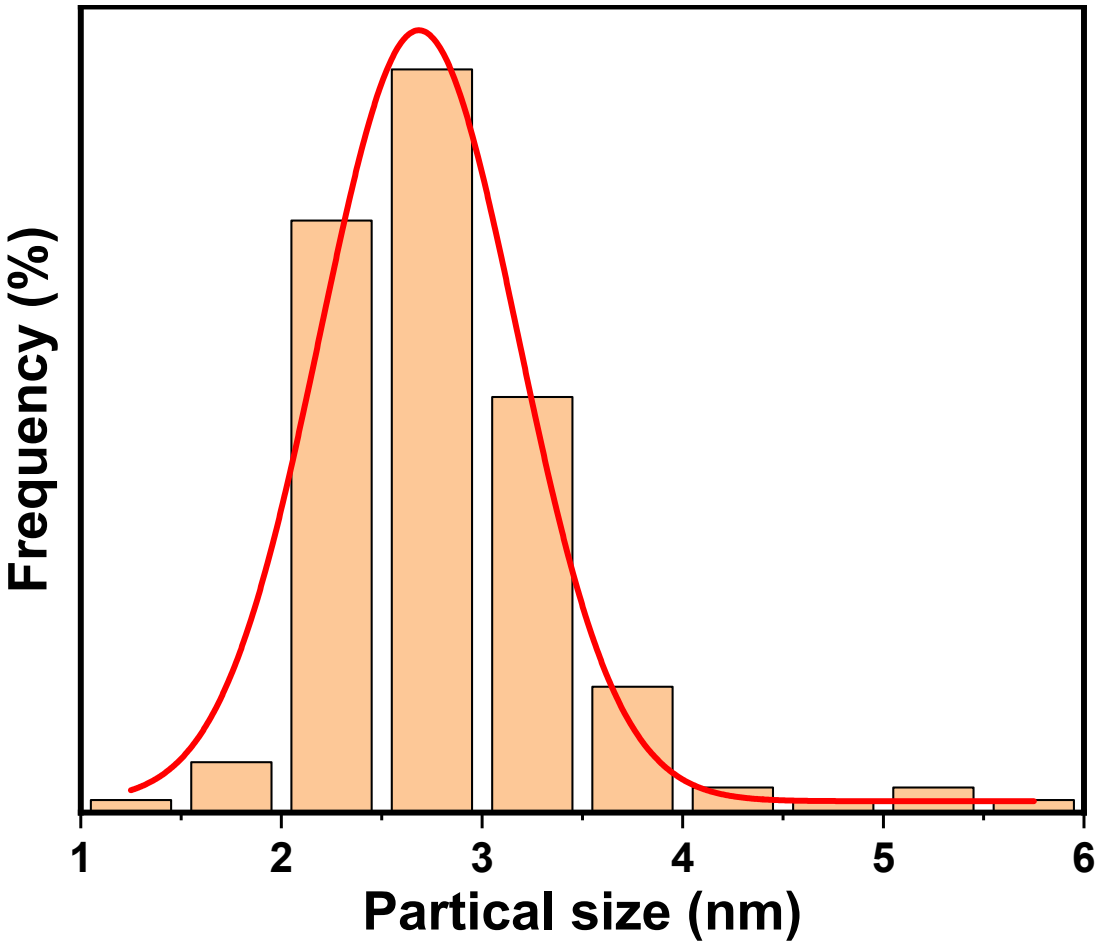

Figure S12. The particle size distribution histogram of R-C-dots.

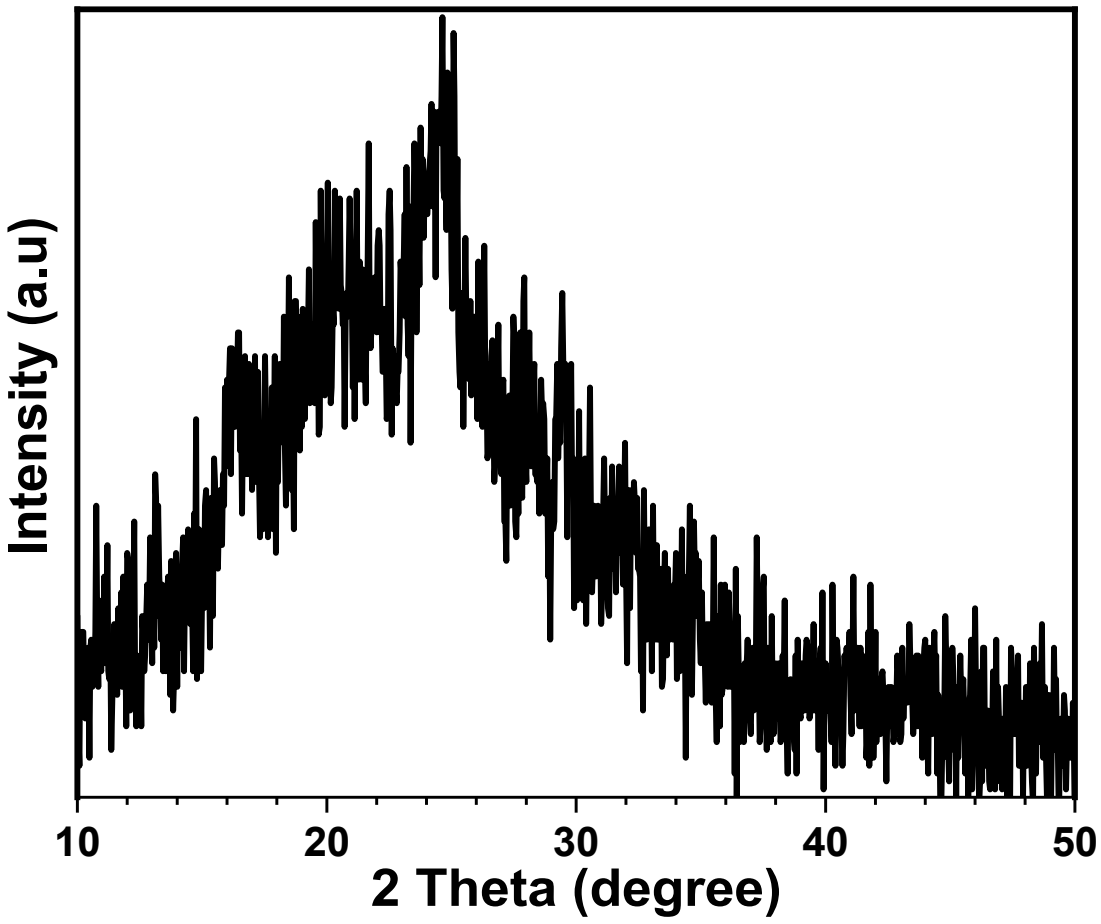

Figure S13. The XRD pattern of R-C-dots.

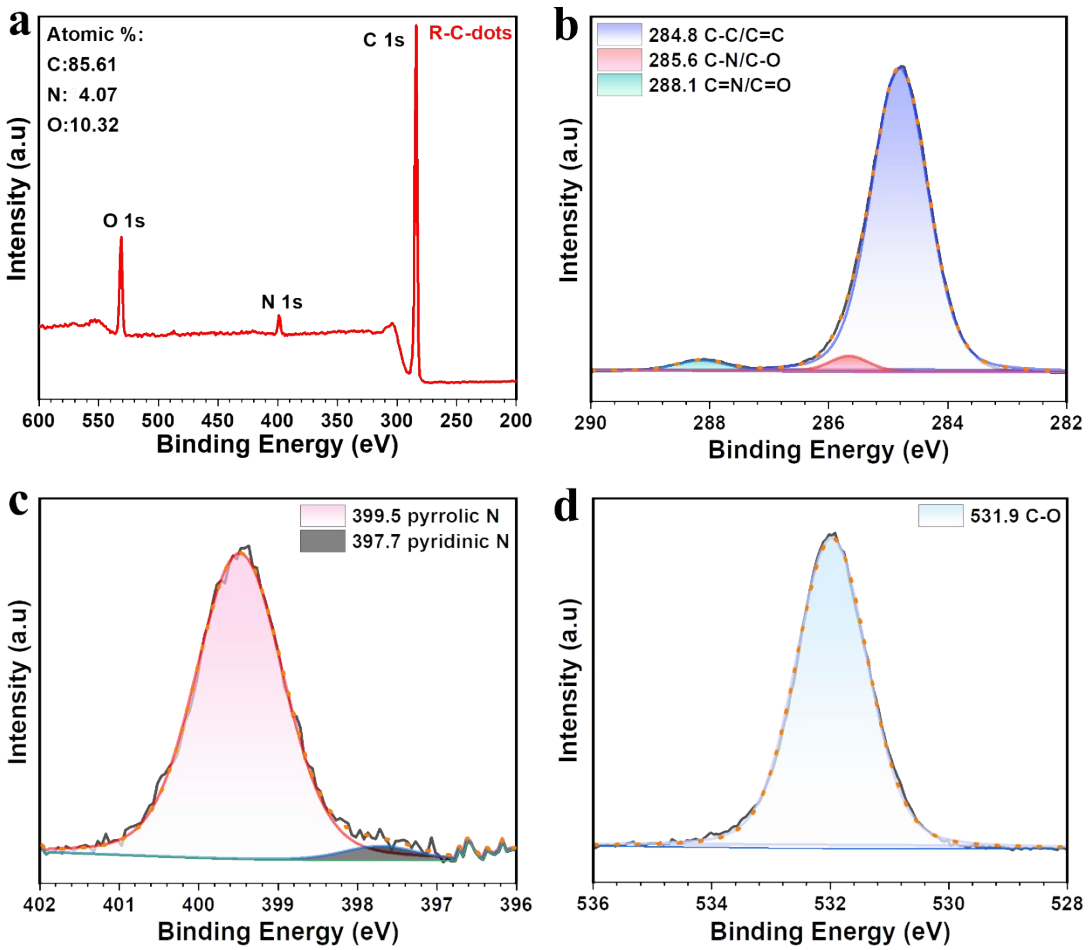

Figure S14. XPS analysis of R-C-dots. (a) Full-scan XPS spectrum of R-C-dots. (b)-(d) High-resolution XPS C 1s, N 1s, and O 1s spectra of R-C-dots.

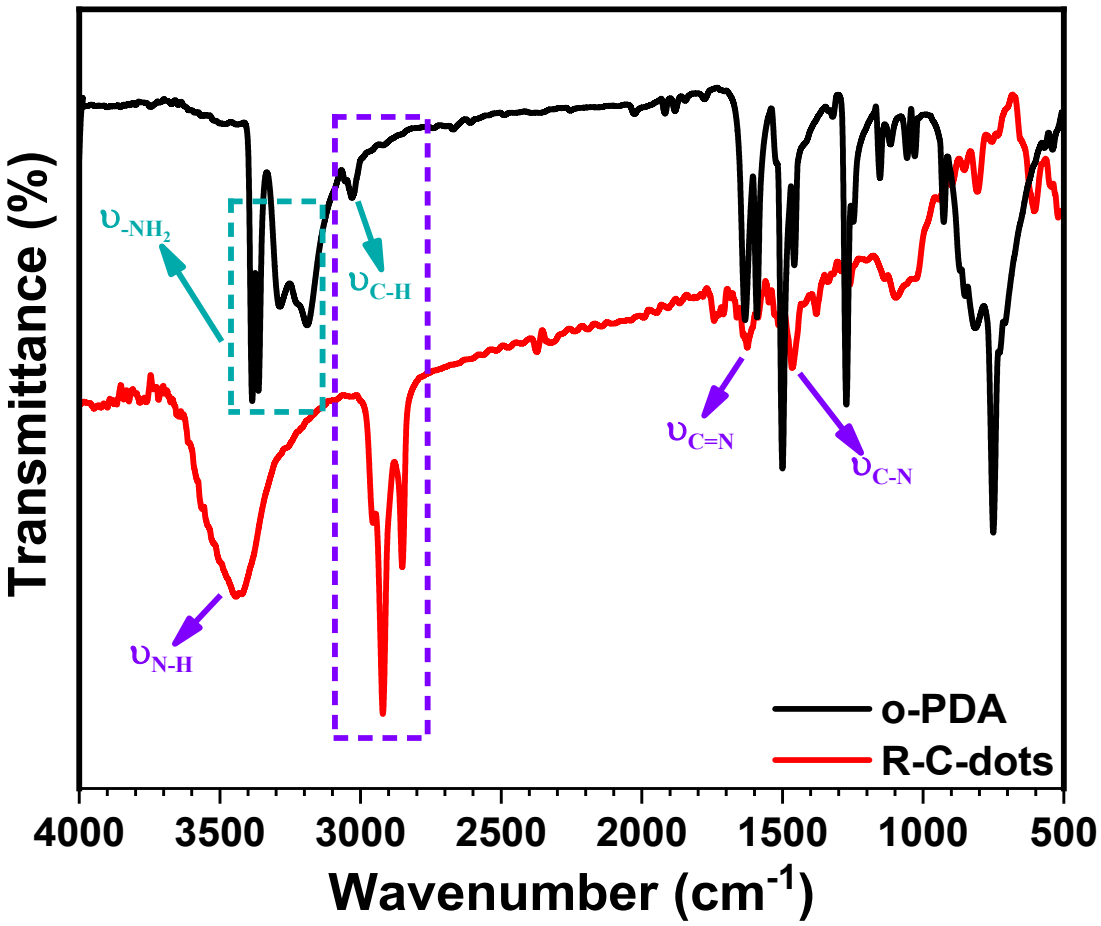

Figure S15. The FTIR spectra of R-C-dots and o-PDA.

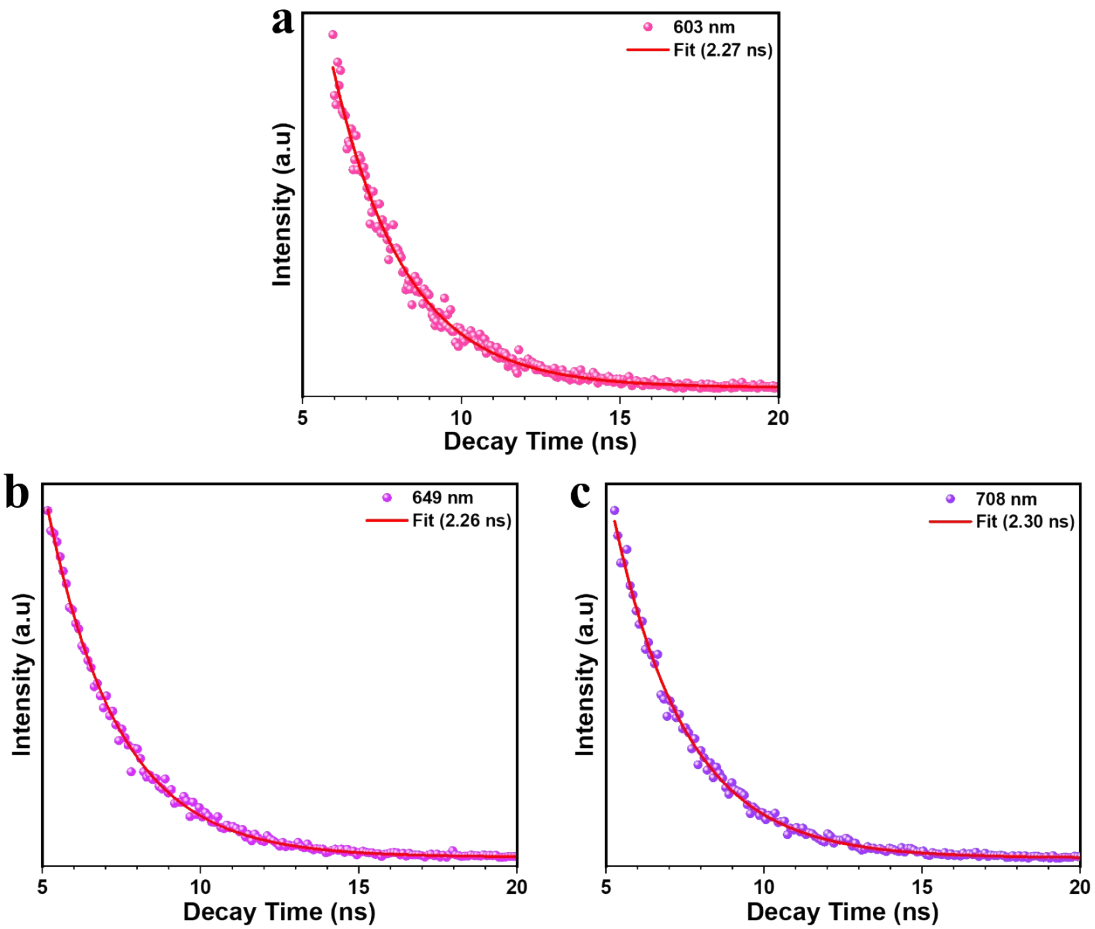

Figure S16. PL decay curves of R-C-dots with emissions located at 603 nm (a), 649 nm (b), and 708 nm (c), respectively.

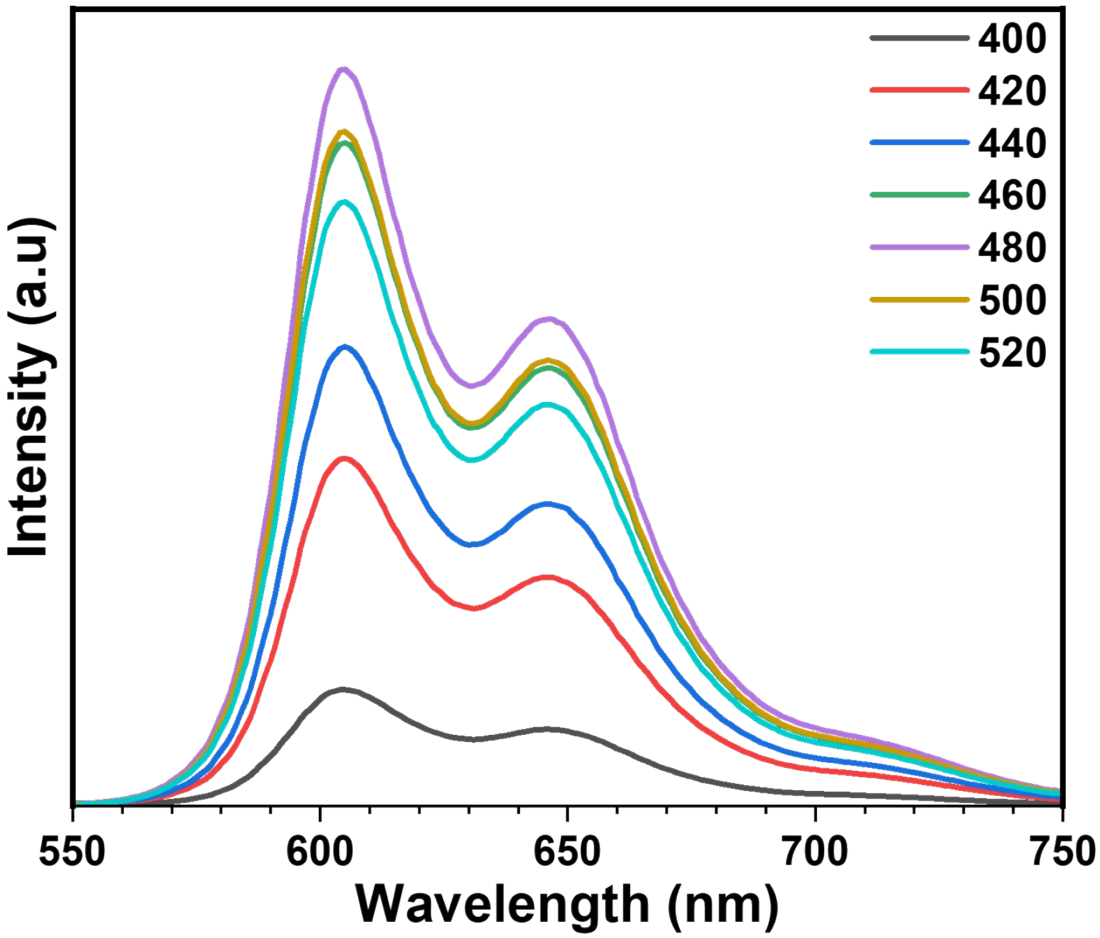

Figure S17. The PL spectra of R-C-dots under different excitation wavelengths.

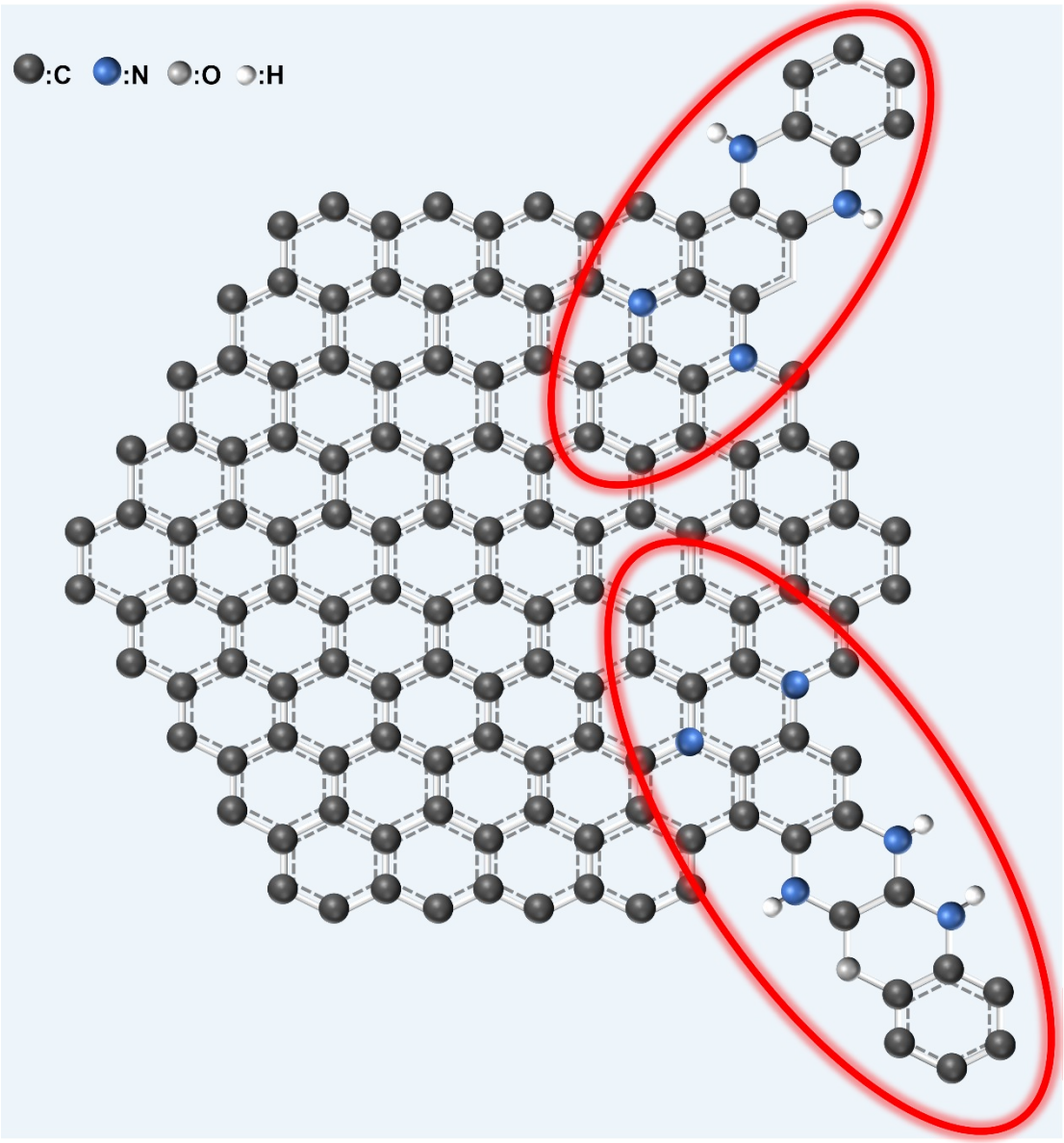

Figure S18. Schematic diagram of DHQP molecules, which are embedded in C-dots.

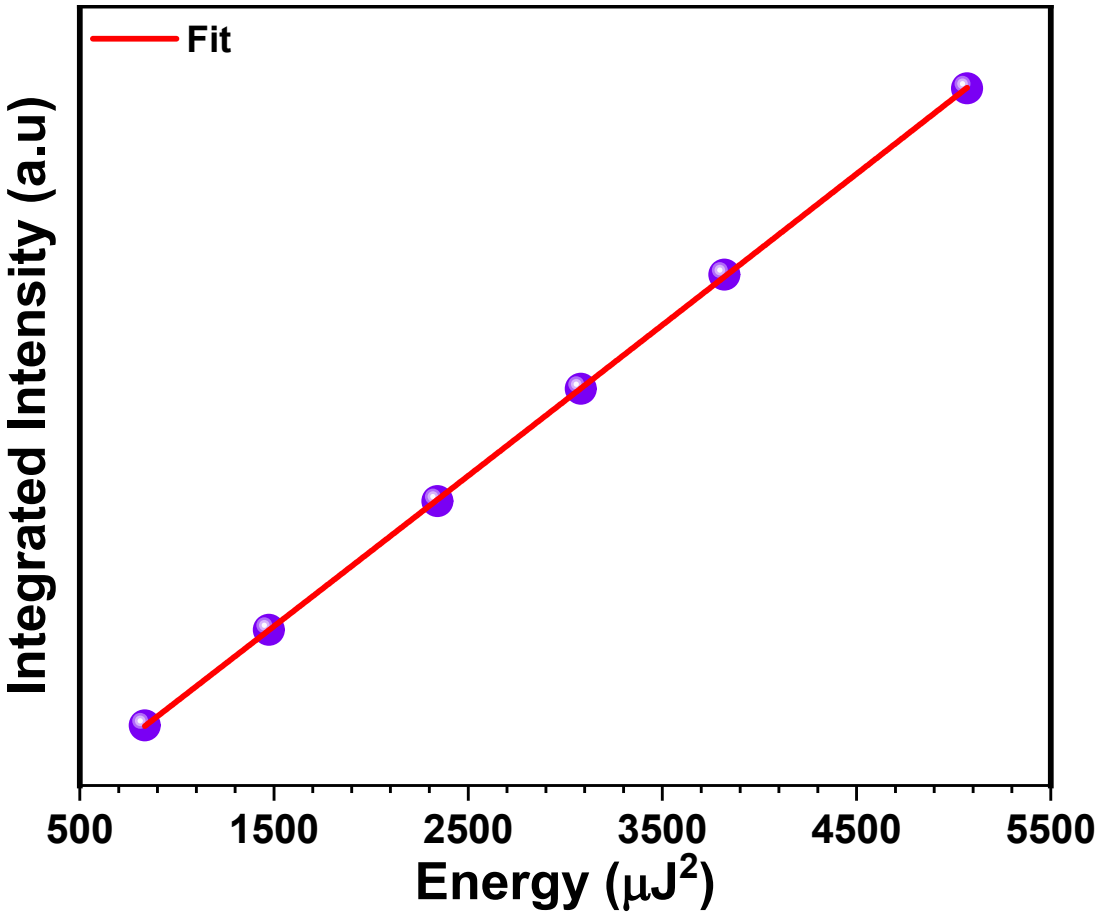

Figure S19. Relationship between the two-photon emission intensity and the square of laser power.

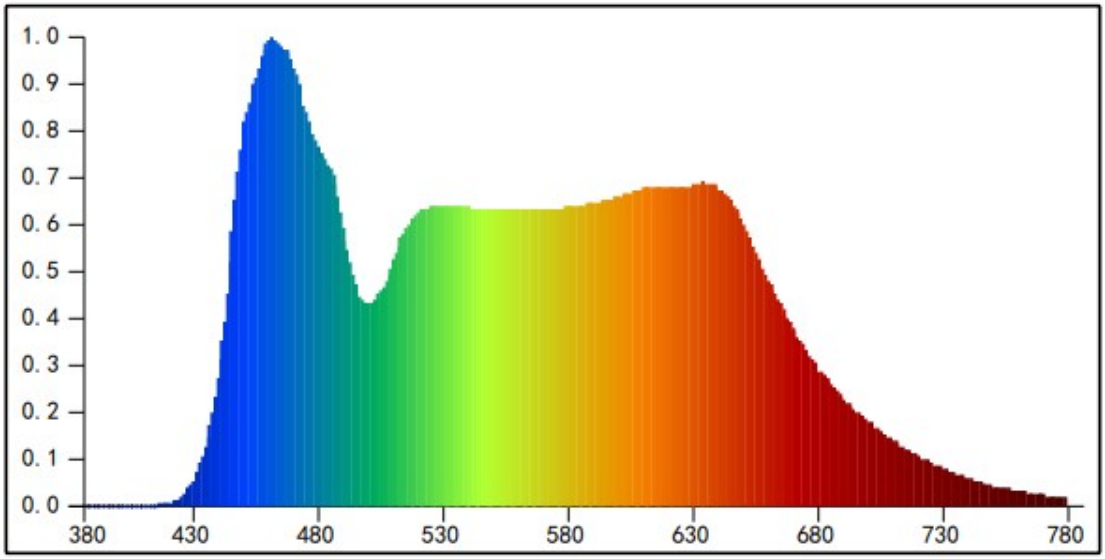

Figure S20. PL spectra of WLED excited by 3 mA direct current.

Red, green, blue ratios is 34.1 %, 39.5 %, and 26.5 %, respectively.

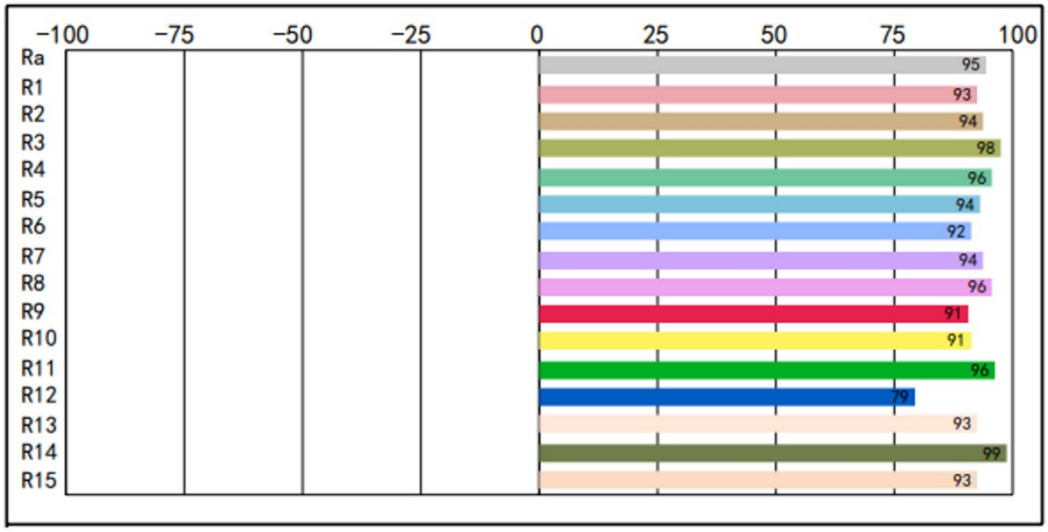

Figure S21. The color rendering parameters (R1-R15) of the WLED.

Table S3. Optimizations of WLED based on different C-dots.

CIE	CRI	CCT (k)	References
(0.41,0.38)	92.7	3827	*Adv. Optical Mater.*[1]
(0.28,0.29)	86.7	5994	*Sci. Adv.*[2]
(0.33,0.36)	88	5452	*Adv. Sci.*[3]
(0.41,0.40)	94.8	3542	*Angew. Chem. Int. Ed.*[4]
(0.34, 0.38)	82	5028	*J. Mater. Chem. C.*[5]
(0.39, 0.37)	91.5	3723	*ACS Appl. Nano Mater.*[6]
(0.29, 0.31)	88	8588	*Carbon.*[7]
(0.33, 0.36)	86.4	5416	*Nano Res.*[8]
(0.33, 0.36)	97	6007	*Adv. Sci.*[9]
(0.32, 0.35)	90.1	5282	*Adv. Funct. Mater.*[10]
(0.33, 0.38)	92.9	6824	*J. Colloid Interface Sci.*[11]
(0.43, 0.40)	97	2988	*Small.*[12]
(0.32, 0.33)	92	5227	*Chem. Eng. J.* [13]
(0.33, 0.33)	94.5	5432	This work

REFERENCES

1 X. Zhang, H. Yang, Z. Wan, T. Su, X. Zhang, J. Zhuang, B. Lei, Y. Liu and C. Hu, Self-quenching-resistant red emissive carbon dots with high stability for warm white light-emitting diodes with a high color rendering index, *Adv. Optical Mater.*, 2020, **8**, 2000251.

2 L. Wang, W. -T. Li, L. -Q. Yin, Y. -J. Liu, H. -Z. Guo, J. -W. Lai, Y. Han, G. Li, M. Li, J. -H. Zhang, R. Vajtai, P. -M. Ajayan and M. -H. Wu, Full-color fluorescent carbon quantum dots, *Sci. Adv.*, 2020, **6**, eabb6772.

3 B. Wang, J. Yu, L. Sui, S. Zhu, Z. Tang, B. Yang and S. Lu, Rational design of multi-color-emissive carbon dots in a single reaction system by hydrothermal, *Adv. Sci.*, 2020, **8**, 2001453.

4 T. Meng, Z. Wang, T. Yuan, X. Li, Y. Li, Y. Zhang and L. Fan, Gram-scale synthesis of highly efficient rare-earth-element-free red/green/blue solid-state bandgap fluorescent carbon quantum rings for white light-emitting diodes, *Angew. Chem. Int. Ed.*, 2021, **60**, 16343-16348.

5 Q. Li, Y. Li, S. Meng, J. Yang, Y. Qin, J. Tan and S. Qu, Achieving 46% efficient white-light emissive carbon dot-based materials by enhancing phosphorescence for single-component white-light-

emitting diodes, *J. Mater. Chem. C.*, 2021, **9**, 6796–6801.

6 Q. Han, W. Xu, C. Ji, G. Xiong, C. Shi, D. Zhang, W. Shi, Y. Jiang and Z. Peng, Multicolor and single-component white light-emitting carbon dots from a single precursor for light-emitting diodes, *ACS Appl. Nano Mater.*, 2022, **5**, 15914-15924.

7 J. Wang, J. Zheng, Y. Yang, X. Liu, J. Qiu and Y. Tian, Tunable full-color solid-state fluorescent carbon dots for light emitting diodes, *Carbon*, 2022, **190**, 22-31.

8 H. Ding, X. -X. Zhou, Z. -H. Zhang, Y. -P. Zhao, J. -S. Wei and H. -M. Xiong, Large scale synthesis of full-color emissive carbon dots from a single carbon source by a solvent-free method, *Nano Res.*, 2021, **15**, 3548-3555.

9 Z. Yan, T. Chen, L. Yan, X. Liu, J. Zheng, F. -D. Ren, Y. Yang, B. Liu, X. Liu and B. Xu, One-step synthesis of white-light-emitting carbon dots for white LEDs with a high color rendering index of 97, *Adv. Sci.*, 2023, **10**, 2206386.

10 Y. Ma, L. Wu, X. Ren, Y. Zhang and S. Lu, Toward kilogram-scale preparation of full-color carbon dots by simply stirring at room temperature in air, *Adv. Funct. Mater.*, 2023, **33**, 2305867.

11 X. Wang, J. Hu, H. Wei, Z. Li, J. Liu, J. Zhang and S. Yang, Ultra-

fast solvent-free protocol remodels the large-scale synthesis of carbon dots for nucleolus-targeting and white light-emitting diodes, *J. Colloid Interface Sci.*, 2023, ***649***, 785-794.

12 W. Xu, Q. Han, C. Ji, F. Zeng, X. Zhang, J. Deng, C. Shi and Z. Peng, Solid-state, hectogram-scale preparation of red carbon dots as phosphor for energy-transfer-induced high-quality white LEDs with CRI of 97, *Small*, 2023, **19**, 2304123.

13 H. Ding, R. Zhao, Z. -H. Zhang, J. -J. Yang, Z. Wang, L. -L. Xiao, X. -H. Li, X. -J. He and H. -M. Xiong, Kilogram-scale synthesis of carbon dots with high-efficiency full-color solid-state fluorescence using an aggregation-induced emission strategy, *Chem. Eng. J.*, 2023, **476**, 146405.